Struct Multidisc Optim (2013) 48:927–938
DOI 10.1007/s00158-013-0997-3

RESEARCH PAPER

Optimization of stresses in a local region for the maximization of sensitivity and minimization of cross—sensitivity of piezoresistive sensors

Qi Xia · Tielin Shi · Shiyuan Liu · Michael Yu Wang

Received: 24 March 2013 / Revised: 12 August 2013 / Accepted: 8 September 2013 / Published online: 28 September 2013

Abstract Based on the analysis of a typical configuration of piezoresistive sensors, the intensity and uniformity of stresses produced by measurand force in the piezoresistive elements are identified as the parameters that affect the sensitivity of a sensor, and stresses produced by perturbation forces in the piezoresistive elements are identified as the parameters that affect the cross-sensitivity of a sensor. To maximize sensitivity and minimize cross-sensitivity, a shape and topology optimization problem is formulated to tailor the stresses in a local region where the piezoresistive elements are placed. In the optimization, the measurand force and perturbation forces are considered separately as two load cases. The optimization problem is solved via the level set based method. Numerical examples in two dimensions are investigated.

Keywords Topology optimization · Stress · Piezoresistive sensor · Sensitivity · Cross-sensitivity

Q. Xia · T. Shi (✉) · S. Liu
The State Key Laboratory of Digital Manufacturing Equipment and Technology, Huazhong University of Science and Technology, Wuhan, China
e-mail: tlshi@mail.hust.edu.cn

M. Y. Wang (✉)
Department of Mechanical and Automation Engineering, The Chinese University of Hong Kong, Shatin, NT, Hong Kong
e-mail: yuwang@mae.cuhk.edu.hk

1 Introduction

The sensing principle of piezoresistive sensors is the well-known piezoresistive effect, i.e., the resistivity changes when a material is subject to stress. In a piezoresistive sensor, an external force deforms a flexible structure and produces stress in piezoresistors. Due to the stress, resistance of the piezoresistors changes, and such change of resistance is transduced to a voltage output.

A good piezoresistive sensor should be sensitive to the external force that is to be measured but should be insensitive to perturbation forces. In other words, a sensor should have high sensitivity to the measurand force but should have low cross-sensitivity to the perturbations. The true meaning of the word "perturbation" depends on the application in question. In a sensor that measures forces in one direction, any other forces in a different direction constitute the perturbation. On the other hand, in a sensor that measures forces in several different directions, the meaning of perturbation is more complicated. In the present study, only sensors that measure one force in one direction are considered.

The over-all sensitivity and cross-sensitivity of a piezoresistive sensor is determined by many factors. First, the sensitivity of the flexible structure determines how much stress will be produced in the piezoresistors. Second, the sensitivity of the piezoresistive material determines how much change of resistance will be produced. Third, the sensitivity of the circuit determines how much voltage will be produced by the change of resistance. Therefore, in order to improve the overall sensitivity, one needs a sensitive mechanical structure, a sensitive material, and a sensitive circuit. The methods to reduce the cross-sensitivity are similar.

The objective of our present study is to design a mechanical structure that is sensitive to the measurand force but insensitive to the perturbation forces. In the literature, insight gained from engineering experiences has been exploited in the design of piezoresistive sensors in order to maximize sensitivity and minimize cross-sensitivity.

First, in order to enhance the sensitivity, the concept of *stress concentration region* (SCR) is introduced into sensors to amplify the stresses in the piezoresistors (Bashir et al. 2000; Yang et al. 2003; Khaled et al. 2003; Yang and Yin 2007; Wang et al. 2011; Zhao et al. 2012; Shi et al. 2012). Bashir et al. (2000) and Yang et al. (2003), Khaled et al. (2003) introduced SCRs in a cantilever. Yang and Yin (2007) used a stripe pattern in a cantilever. Slit feature was used by Wang et al. (2011), Zhao et al. (2012), and Shi et al. (2012).

Beside such human practice of using SCR to enhance sensitivity of sensors, for thousands of years nature insects have been using such a strategy. Holes, grooves, or groups of them are used to increase the deformation or strain of sensing organs, which can be readily found in the exoskeleton of cockroach and fly. Readers are referred to Fratzl and Barth (2009), Vincent et al. (2007), Sane and McHenry (2009) and the references therein.

Second, in order to minimize the stress produced by perturbations, the concepts of *stress isolation* and *stress relaxation* are introduced into the design. Hsieh et al. (2011) used a groove or the so-called guard-ring in a three-axis piezoresistive accelerometer to cut off the transmission path of perturbation forces. Kazama et al. (2013) used a compliant ring-shaped structure to reduce the stress produced by perturbations in piezoresistors of a three-axis accelerometer.

Third, it is very interesting to note that two parallel grooves were ingeniously used by Mohammed et al. (2010) in a strain sensor to simultaneously amplify the stress in one direction but minimize the stress in the perpendicular direction, thus maximizing the sensitivity and minimizing the cross-sensitivity.

The success of the above-mentioned studies demonstrated the effectiveness of using structure features to locally amplify or reduce stresses to enhance the performance of piezoresistive sensors. However, there lacks a systematic and automatic method for such purpose. In order to deal with this issue, a shape and topology optimization based approach is investigated in the present study. Based on the analysis of a typical configuration of piezoresistive sensors, an optimization problem is formulated. The objective of the shape and topology optimization comprises both maximization of sensitivity and minimization of cross-sensitivity.

Shape and topology optimization based approach has been applied to design piezoresistive sensors (Pedersen 2004; Rubio et al. 2008; Takezawa et al. 2010; Mello et al. 2012; Li and Wang 2012; Xia et al. 2013). Pedersen (2004) optimized a cantilever piezoresistive bio-probe. Rubio et al. (2008) maximized change of resistivity by optimizing a structure to which the piezoresistors are bonded. Takezawa et al. (2010) optimized single—and multi-axis load cells. Mello et al. (2012) optimized piezoresistive plate-based sensors. In our previous study (Xia et al. 2013), stresses in a local region is optimized to enhance the sensitivity. Also, in our previous study (Li and Wang 2012), the von Mises stress in a local region is driven to a value close to zero. The present paper extends the previous studies by considering both the maximization of sensitivity and minimization of cross-sensitivity of a typical configuration of piezoresistive sensors.

The paper is organized as follows. In Section 2 a typical configuration of piezoresistive sensor is analyzed. In Section 3 formulation of the shape and topology optimization problem is described. In Section 4 sensitivity analysis for the optimization problem is described and discussed. In Section 5 the level set method is briefly described. Section 6 gives numerical examples and discussions. Section 7 concludes this paper.

2 A typical configuration of piezoresistive sensors

The typical configuration of piezoresistive sensors considered in the present study is similar to that of our previous study (Xia et al. 2013). For the convenience of readers, some details are rewritten here. For a piezoresistor whose area is A_R, the normalized change of resistance is given by Bashir et al. (2000), Mohammed et al. (2010), Xia et al. (2013)

$$\left.\frac{\Delta R}{R}\right|_{\text{unit load}} = \frac{1}{A_R}\int_0^{A_R} (\pi_l \sigma_l + \pi_t \sigma_t)\,\mathrm{d}x \tag{1}$$

where π_l is the piezoresistive coefficient for the stress σ_l in the direction of electrical current, π_t is the piezoresistive coefficient for the stress σ_t perpendicular to the direction of electrical current. The subscript "unit load" in (1) is omitted in the following.

For the doped silicon of the present study, π_l and π_t depend on the orientation of a piezoresistor in the crystallographic axes of a silicon substrate (Liu 2006). When the longitudinal direction of a piezoresistor is oriented along the $\langle 110\rangle$ directions of a (100) silicon wafer under the plane stress state, $\Delta R/R$ is the highest (Smith 1954), and the π_l and π_t are given by Liu (2006)

$$\pi_l = (\pi_{11} + \pi_{12} + \pi_{44})/2 \tag{2}$$

$$\pi_t = (\pi_{11} + \pi_{12} - \pi_{44})/2 \tag{3}$$

A typical configuration of the Wheatstone bridge is illustrated in Fig. 1. In such a configuration the x and y axes are respectively aligned to the [110] and [$\bar{1}$10] direction of the

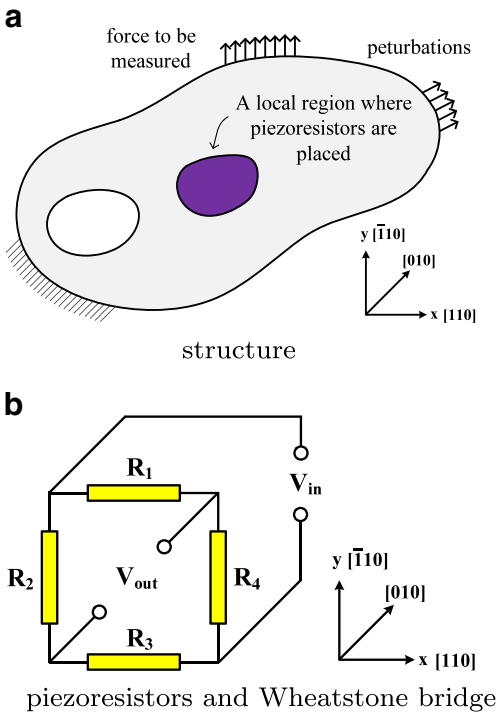

Fig. 1 A typical configuration of piezoresistive sensor

silicon substrate. All the piezoresistors are placed in a single local region and subject to stresses: σ_l of R_1 and R_3 is σ_{xx}; σ_t of them is σ_{yy}; σ_l of R_2 and R_4 is σ_{yy}; σ_t of them is σ_{xx}.

The normalized changes of resistance are given by

$$\frac{\Delta R_i}{R_i} = \frac{1}{2A_R}\int_0^{A_R}\left[(\pi_{11}+\pi_{12})(\sigma_{xx}+\sigma_{yy}) + \pi_{44}(\sigma_{xx}-\sigma_{yy})\right]\mathrm{d}x,\ i=1,3 \quad (4)$$

$$\frac{\Delta R_i}{R_i} = \frac{1}{2A_R}\int_0^{A_R}\left[(\pi_{11}+\pi_{12})(\sigma_{xx}+\sigma_{yy}) - \pi_{44}(\sigma_{xx}-\sigma_{yy})\right]\mathrm{d}x,\ i=2,4 \quad (5)$$

Since π_{11} and π_{12} are very small as compared to π_{44}, the term $\pi_{44}(\sigma_{xx}-\sigma_{yy})$ has a dominant role in (4) and (5), and the term $(\pi_{11}+\pi_{12})(\sigma_{xx}+\sigma_{yy})$ can be neglected (Mohammed et al. 2010; Xia et al. 2013).

When a piezoresistor is very small, the stresses σ_l and σ_t in it are regarded as uniform and treated as constants. As a result, one arrives at simplified relations as Mohammed et al. (2010) and Xia et al. (2013)

$$\frac{\Delta R_i}{R_i} = \frac{1}{2}\left[(\pi_{11}+\pi_{12})(\sigma_{xx}+\sigma_{yy}) + \pi_{44}(\sigma_{xx}-\sigma_{yy})\right],\ i=1,3 \quad (6)$$

$$\frac{\Delta R_i}{R_i} = \frac{1}{2}\left[(\pi_{11}+\pi_{12})(\sigma_{xx}+\sigma_{yy}) - \pi_{44}(\sigma_{xx}-\sigma_{yy})\right],\ i=2,4 \quad (7)$$

This assumption of uniformity of stresses simplifies the mathematical model of the sensitivity and calibration of the sensor. However, in the present study, such an assumption cannot be taken into the optimization. In other words, if the uniformity of stresses is not explicitly considered in the optimization, the resulting stresses will probably not be uniform (Xia et al. 2013). Therefore, the optimization problem should be formulated to drive the stresses to be uniform.

When the stresses are uniform and the term $(\pi_{11}+\pi_{12})(\sigma_{xx}+\sigma_{yy})$ in (4) and (5) is neglected, the ratio between the output and input voltage is given by Mohammed et al. (2010) and Xia et al. (2013)

$$\frac{V_{out}}{V_{in}} = \frac{\pi_{44}}{2}(\sigma_{xx}-\sigma_{yy}) \quad (8)$$

Equation (8) gives the voltage output produced by external forces which comprise both the measurand force and the perturbation forces, as shown in Fig 1. Due to the linearity of linear elasticity, we see that (8) can be rewritten as a superposition of two parts

$$\frac{V_{out}}{V_{in}} = \frac{\pi_{44}}{2}\left(\sigma_{xx}^m-\sigma_{yy}^m\right) + \frac{\pi_{44}}{2}\left(\sigma_{xx}^p-\sigma_{yy}^p\right) \quad (9)$$

where the superscript m means the measurand, and the superscript p means the perturbation. As can be seen in (9), the sensitivity of the sensor depends on the absolute value of stress differential $\sigma_{xx}^m-\sigma_{yy}^m$. Therefore, the absolute value of $\sigma_{xx}^m-\sigma_{yy}^m$ should be maximized to enhance the sensitivity. The cross-sensitivity depend on the absolute value of $\sigma_{xx}^p-\sigma_{yy}^p$, and the absolute value of $\sigma_{xx}^p-\sigma_{yy}^p$ should be minimized to reduce the cross-sensitivity. In addition, considering the safety of the sensor structure, the maximum stress should be below an admissible level.

3 Optimization problem

3.1 Formulation of problem

Let $\Omega \subset \mathbb{R}^2$ denote the region occupied by the flexible structure of a piezoresistive sensor. It is required that during the optimization Ω stay in a fixed reference domain $D \subset \mathbb{R}^2$, i.e., $\Omega \subset D$. Suppose that all the piezoresistors are placed in a local region $\Omega_1 \subset \Omega$. In the present study, the local region Ω_1 is fixed during the optimization. In addition, we denote the rest region of the structure as Ω_0, i.e.,

$$\Omega_0 = \Omega \backslash \Omega_1 \quad (10)$$

In the present study, the measurand force (denoted as t_m) and a perturbation force (denoted as t_p) are considered as

two different load cases. If there are more than one perturbation forces, they are considered as many different load cases. For the load case of t_m, suppose that the boundary of Ω consists of three disjoint parts, i.e.,

$$\partial\Omega = \Gamma_D \cup \Gamma_N^m \cup \Gamma_H^m \tag{11}$$

where the structure is fixed on Γ_D; the force t_m is applied on the Neumann boundary Γ_N^m; Γ_H^m is traction free. For the load case of perturbation force t_p, we assume in the present study that Γ_N^p where t_p is applied is fixed and not subject to optimization. Such an assumption is reasonable because if Γ_N^p can be changed, the cross-sensitivity can be simply eliminated by disconnecting the structure from the perturbation force t_p. Because the local region Ω_1, the boundaries Γ_N^m and Γ_N^p are fixed during the optimization, the boundary that is free to move is

$$\Gamma_O = \Gamma_H^m \backslash (\partial\Omega_1 \cup \Gamma_N^p) \tag{12}$$

The displacements induced by an external force (body force is neglected in the present study) is the solution to a linear elasticity equation whose weak form is given as

$$a(u, v) = \ell(v), \ \forall\, v \in U \tag{13}$$

where $U = \{v \in H^1(\Omega)^d \mid v = 0 \text{ on } \Gamma_D\}$ is the space of kinematically admissible displacement fields, and $a(u, v)$ and $\ell(v)$ are defined as

$$a(u, v) = \int_\Omega Ae(u) \cdot e(v)\, \mathrm{d}x \tag{14}$$

$$\ell(v) = \int_{\Gamma_N} t\, v\, \mathrm{d}s \tag{15}$$

where A describes the Hooke's law; $e(u)$ is the strain tensor; $\sigma(u) = A\, e(u)$ is the stress tensor; t is the boundary traction force.

As mentioned in Section 2, according to the safety requirement, at each point in a structure the stress should be below an admissible level, i.e.,

$$\sigma_v\,(u(x)) \le \sigma_a, \ \forall x \in \Omega \tag{16}$$

where σ_a is the admissible stress of the material; σ_v is the von Mises stress, and in the plane stress state it is given by

$$\sigma_v = \sqrt{\sigma_{xx}^2 + \sigma_{yy}^2 - \sigma_{xx}\sigma_{yy} + 3\sigma_{xy}^2} \tag{17}$$

Based on the analysis in Section 2, an optimization problem is formulated. In fact, there are many possible formulations of the optimization problem, and a simple one is given by

$$\begin{aligned} \min\ & J = \textstyle\sum_{i=0}^{5} g_i + \beta A \\ \text{s.t.}\ & a(u_m, v_m) = \ell(v_m),\ \forall v_m \in U \\ & a(u_p, v_p) = \ell(v_p),\ \forall v_p \in U \end{aligned} \tag{18}$$

where u_m denotes the displacement field due to the measurand force t_m; u_p denotes the displacement field due to perturbation force t_p; $\beta > 0$ is a weight parameter; $A = \int_\Omega \mathrm{d}x$ is the area of the 2D region Ω; functions g_i in the objective function J are given by

$$g_0 = \int_{\Omega_0} \sigma_v^2(u_m)\,[1 + \alpha H\,(\sigma_v(u_m) - \overline{\sigma}_0)]\ \mathrm{d}x \tag{19}$$

$$g_1 = w_1 \int_{\Omega_1} [\sigma_v(u_m) - \overline{\sigma}]^2\ \mathrm{d}x \tag{20}$$

$$g_2 = w_2 \int_{\Omega_1} [\sigma_{xx}(u_m) - \overline{\sigma}]^2\ \mathrm{d}x \tag{21}$$

$$g_3 = w_3 \int_{\Omega_1} \sigma_{yy}^2(u_m)\, \mathrm{d}x \tag{22}$$

$$g_4 = w_4 \int_{\Omega_0} \sigma_v^2(u_p)\left[1 + \alpha H\left(\sigma_v(u_p) - \overline{\sigma}_0\right)\right] \mathrm{d}x \tag{23}$$

$$g_5 = w_5 \int_{\Omega_1} \sigma_v^2(u_p)\, \mathrm{d}x \tag{24}$$

where $\overline{\sigma}_0$ and $\overline{\sigma}$ in the function g_i are parameters specified before optimization, and they should be smaller than the admissible stress of the material, i.e, $0 < \overline{\sigma}_0 < \sigma_a$ and $0 < \overline{\sigma} < \sigma_a$; $w_i > 0$ are weight parameters. In fact, there are many alternative definitions of g_2 and g_3, and they are discussed in Xia et al. (2013).

Functions g_0 and g_4 are used to deal with the safety requirement given in (16). Function g_0 is a measure of the stresses produced by t_m in Ω_0, and function g_4 is a measure of the stresses produced by t_p in Ω_0. Note that the two integrations are defined for region Ω_0 and that they do not involve with stresses in Ω_1. The measure of stress was proposed and discussed in our previous studies (Xia et al. 2012, 2013). The function H is the Heaviside function, and in practical numerical implementation it is approximated by continuous functions (Xia et al. 2012). According to the Heaviside function, $\overline{\sigma}_0$ in g_0 and g_4 can be regarded as a threshold of von Mises stress above which the stress is penalized, and the parameter α controls the weight of penalization (Xia et al. 2012).

Functions g_1, g_2, g_3 are used to maximize the sensitivity, and function g_5 is used to minimized the cross-sensitivity. They are discussed in detail in the following sections.

3.2 Discussions on maximization of sensitivity

Function g_1 is used to drive $\sigma_v(u_m)$ to $\overline{\sigma}$ at each point in Ω_1, which also ensures the safety of structure because $0 < \overline{\sigma} < \sigma_a$. Function g_2 is used to drive $\sigma_{xx}(u_m)$ to $\overline{\sigma}$ and ensure the uniformity of $\sigma_{xx}(u_m)$ in Ω_1. Function g_3 is used to drive $\sigma_{yy}(u_m)$ to zero and ensure the uniformity.

More importantly, when $\sigma_v(u_m) = \overline{\sigma}$ and $\sigma_{yy}(u_m) = 0$ at a point, according to (17), the maximal and minimal value of $\sigma_{xx}(u_m)$ that can be achieved at the point are respectively $\overline{\sigma}$ and $-\overline{\sigma}$, therefore the function g_2 maximizes $\sigma_{xx}(u_m)$ in Ω_2. Now, in Ω_1 the stresses are: $\sigma_{xx}(u_m) = \overline{\sigma}$, $\sigma_{yy}(u_m) = 0$. Viewing (9), one can see that the sensitivity is maximized.

Although the sensor considered in the present study measures only one force in one direction, the direction of the single force often changes in real engineering applications, as shown in Fig. 2. It seems that two load cases of measurand forces should be considered in the formulation of the optimization, because it is well known that the optimal structure obtained by shape and topology optimization is optimal only for the force that is formulated in the definition of optimization problem. However, based on the linearity elasticity assumption, it can be readily shown that the formulation of the optimization problem given by (18) is able to deal with two different measurand forces that have the same magnitude but opposite directions.

3.3 Discussions on minimization of cross-sensitivity

Function g_5 in (24) is used to drive $\sigma_v(u_p)$ to zero at each point in Ω_1, thus minimizing the stresses $\sigma_{xx}(u_p)$ and $\sigma_{yy}(u_p)$ produced by the perturbation force and in turn minimizing the cross-sensitivity, as shown in (9).

Function g_5 can be alternatively defined as $g_5 = w_5 \int_{\Omega_1} [\sigma_{xx}(u_p) - \sigma_{yy}(u_p)]^2 \mathrm{d}x$. This alternative definition drives $\sigma_{xx}(u_p) - \sigma_{yy}(u_p)$ to zero at each point in Ω_1, which also minimizes the cross-sensitivity. However, from the view point of sensor design, (24) is more appropriate because it ensures the piezoresistors in the local region Ω_1 are minimally affected by the perturbation force.

In the formulation of optimization problem given by (18), only one perturbation force is considered. If there exist more than one perturbation forces, more functions that are similar to g_4 and g_5 should be introduced into the optimization problem to minimize the cross-sensitivity. In a special case where the two perturbation forces have the same magnitude but opposite directions, as shown in Fig. 3, the function g_4 and g_5 are able to minimize the cross-sensitivity for both of the two perturbation forces. The reason is similar to that described in Section 3.2, i.e., the change of direction of the perturbation force will not change the Mises stress σ_v in g_4 and g_5. Finally, the perturbation forces are usually not deterministic, and there exists uncertainty of them, but in the present study such uncertainty about the perturbation forces is not considered.

4 Sensitivity analysis

In this section we describe the sensitivity analysis for the optimization problem (18). The material derivative (Choi and Kim 2005) and the adjoint method are employed. The Lagrangian is

$$\mathscr{L} = J + a(u_m, w_m) - \ell(w_m) + a(u_p, w_p) - \ell(w_p) \quad (25)$$

where $w_m \in U$ and $w_p \in U$ are the Lagrange multipliers for the equations of linear elasticity system (13).

The material derivative of the Lagrangian is given by

$$\mathscr{L}' = J' + a'(u_m, w_m) - \ell'(w_m) + a'(u_p, w_p) - \ell'(w_p) \quad (26)$$

The material derivatives of each term is presented as follows. First,

$$J' = \sum_{i=0}^{5} g_i' + \beta A' \quad (27)$$

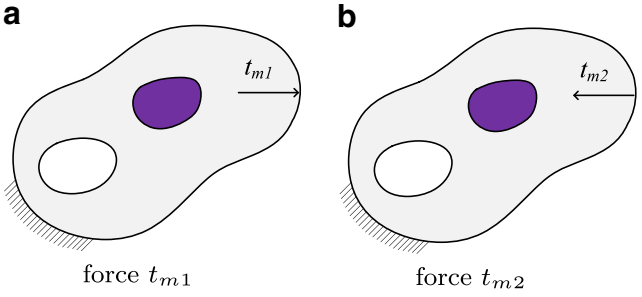

Fig. 2 Two load cases of measurand force

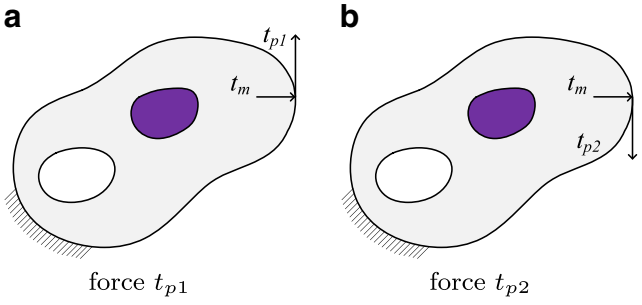

Fig. 3 Two load cases of perturbation force

where $A' = \int_{\partial\Omega} \mathrm{d}s$, and g_i' are given by

$$g_0' = \int_{\Omega_0} 2\sigma_v(u_m)\,\sigma_v'(u_m)\,[1+\alpha H(\sigma_v(u_m)-\overline{\sigma}_0)]\,\mathrm{d}x + \int_{\Omega_0} \alpha\,\sigma_v^2(u_m)\,\delta(\sigma_v(u_m)-\overline{\sigma}_0)\,\sigma_v'(u_m)\,\mathrm{d}x + \int_{\partial\Omega_0} \sigma_v^2(u_m)\,[1+\alpha H(\sigma_v(u_m)-\overline{\sigma}_0)]\,V_n\,\mathrm{d}s \tag{28}$$

$$g_1' = w_1 \int_{\Omega_1} 2\,[\sigma_v(u_m)-\overline{\sigma}]\,\sigma_v'(u_m)\,\mathrm{d}x \tag{29}$$

$$g_2' = w_2 \int_{\Omega_1} 2\,[\sigma_{xx}(u_m)-\overline{\sigma}]\,\sigma_{xx}'(u_m)\,\mathrm{d}x \tag{30}$$

$$g_3' = w_3 \int_{\Omega_1} 2\sigma_{yy}(u_m)\sigma_{yy}'(u_m)\,\mathrm{d}x \tag{31}$$

$$g_4' = w_4 \int_{\Omega_0} 2\sigma_v(u_p)\,\sigma_v'(u_p)\left[1+\alpha H(\sigma_v(u_p)-\overline{\sigma}_0)\right]\mathrm{d}x + w_4 \int_{\Omega_0} \alpha\,\sigma_v^2(u_p)\,\delta(\sigma_v(u_p)-\overline{\sigma}_0)\,\sigma_v'(u_p)\,\mathrm{d}x + w_4 \int_{\partial\Omega_0} \sigma_v^2(u_p)\left[1+\alpha H(\sigma_v(u_p)-\overline{\sigma}_0)\right]V_n\,\mathrm{d}s \tag{32}$$

$$g_5' = w_5 \int_{\Omega_1} 2\sigma_v(u_p)\sigma_v'(u_p)\,\mathrm{d}x \tag{33}$$

where

$$\sigma_v'(u) = \frac{1}{2\sigma_v}\left[2\sigma_{xx}-\sigma_{yy}, 2\sigma_{yy}-\sigma_{xx}, 6\sigma_{xy}\right]\sigma(u') \tag{34}$$

$$\sigma_{xx}'(u) = [1,0,0]\sigma(u') \tag{35}$$

$$\sigma_{yy}'(u) = [0,1,0]\sigma(u') \tag{36}$$

Note that there are no V_n terms in g_1', g_2', g_3', and g_5' because the local region Ω_1 is fixed and its boundary is not subject to optimization.

The derivative $a'(u_m, w_m)$, $\ell'(w_m)$, $a'(u_p, w_p)$, and $\ell'(w_p)$are given by

$$a'(u_m, w_m) = a(u_m', w_m) + a(u_m, w_m') + \int_{\partial\Omega} Ae(u_m)\cdot e(w_m)V_n\mathrm{d}s \tag{37}$$

$$\ell'(w_m) = \ell(w_m') + \int_{\Gamma_N}\left[\nabla(tw_m)^T n + \kappa t w_m\right]V_n\mathrm{d}s \tag{38}$$

$$a'(u_p, w_p) = a(u_p', w_p) + a(u_p, w_p') + \int_{\partial\Omega} Ae(u_p)\cdot e(w_p)V_n\mathrm{d}s \tag{39}$$

$$\ell'(w_p) = \ell(w_p') + \int_{\Gamma_N}\left[\nabla(tw_p)^T n + \kappa t w_p\right]V_n\mathrm{d}s \tag{40}$$

Substitute (27)–(40) into (26), we obtain the material derivative of the Lagrangian.

Collecting all the terms that contain w_m' in $\mathscr{L}'$ and letting the sum of these terms be zero, we recover the weak form of the elasticity equation, that is

$$a(u_m, w_m') = \ell(w_m') \tag{41}$$

Therefore, the terms in $\mathscr{L}'$ that contain w_m' are canceled. Similarly, collecting all the terms that contain w_p' in $\mathscr{L}'$ and letting the sum of these terms be zero, we get

$$a(u_p, w_p') = \ell(w_p') \tag{42}$$

Therefore, the terms in $\mathscr{L}'$ that contain w_p' are canceled.

Collecting all the terms that contain u_m', and letting the sum of these terms be zero, we obtain an adjoint equation, that is

$$\begin{aligned} a(u_m', w_m) = &-\int_{\Omega_0} 2\sigma_v(u_m)\,\sigma_v'(u_m)\,[1+\alpha H(\sigma_v(u_m)-\overline{\sigma}_0)]\,\mathrm{d}x \\ &-\int_{\Omega_0} \alpha\,\sigma_v^2(u_m)\,\delta(\sigma_v(u_m)-\overline{\sigma}_0)\,\sigma_v'(u_m)\,\mathrm{d}x \\ &-w_1\int_{\Omega_1} 2\,[\sigma_v(u_m)-\overline{\sigma}]\,\sigma_v'(u_m)\,\mathrm{d}x \\ &-w_2\int_{\Omega_1} 2\,[\sigma_{xx}(u_m)-\overline{\sigma}]\,\sigma_{xx}'(u_m)\,\mathrm{d}x \\ &-w_3\int_{\Omega_1} 2\sigma_{yy}(u_m)\sigma_{yy}'(u_m)\,\mathrm{d}x,\ \forall u_m' \in U \end{aligned} \tag{43}$$

Collecting all the terms that contain u_p', and letting the sum of these terms be zero, we obtain another adjoint equation, that is

$$\begin{aligned} a(u_p', w_p) = &-w_4\int_{\Omega_0} 2\sigma_v(u_p)\,\sigma_v'(u_p)\left[1+\alpha H(\sigma_v(u_p)-\overline{\sigma}_0)\right]\mathrm{d}x \\ &-w_4\int_{\Omega_0} \alpha\,\sigma_v^2(u_p)\,\delta(\sigma_v(u_p)-\overline{\sigma}_0)\,\sigma_v'(u_p)\,\mathrm{d}x \\ &-w_5\int_{\Omega_1} 2\sigma_v(u_p)\sigma_v'(u_p)\,\mathrm{d}x \end{aligned} \tag{44}$$

Collecting all the terms that contain V_n, and noticing that only Γ_O subjects to optimization, we obtain the shape derivative of the Lagrangian

$$\mathscr{L}' = \int_{\Gamma_O} G\,V_n\,\mathrm{d}s \tag{45}$$

where shape gradient density G is given by

$$\begin{aligned} G = &\sigma_v^2(u_m)\,[1+\alpha H(\sigma_v(u_m)-\overline{\sigma}_0)] \\ &+w_4\sigma_v^2(u_p)\left[1+\alpha H(\sigma_v(u_p)-\overline{\sigma}_0)\right] \\ &\cdot Ae(u_m)\cdot e(w_m) + Ae(u_p)\cdot e(w_p) + \beta \end{aligned} \tag{46}$$

According to (45), we can readily obtain the steepest descent direction by setting

$$V_n(x) = -G(x),\ \forall x \in \Gamma_O \tag{47}$$

It can be seen that such V_n will yield $\mathscr{L}' = -\int_{\Gamma_O} G^2\,\mathrm{d}s \le 0$ which implies the descent of the Lagrangian.

A conjugate mapping (Wang et al. 2004; Mei and Wang 2004) of the velocity V_n is used to speed up the convergence of the optimization as in Xia et al. (2012). To apply the mapping, V_n is first normalized by the maximum value of $|V_n|$, then a mapping given in the following is applied.

$$F(x) = x \exp(1 - |x|) \tag{48}$$

5 The level set method

In the level set method (Sethian 1999; Osher and Fedkiw 2002), the boundary of a shape Ω is represented implicitly through a level set function $\Phi(x)$ as its zero level set, i.e., $\{x \in \mathbb{R}^d \,|\, \Phi(x) = 0\}$ ($d = 2$ or 3), and $\Phi(x)$ can be used to define the inside and outside regions with respect to the boundary as follows

$$\begin{aligned} \Phi(x) = 0 &\iff \forall\, x \in \partial\,\Omega \cap D \\ \Phi(x) < 0 &\iff \forall\, x \in \Omega \\ \Phi(x) > 0 &\iff \forall\, x \in (D \backslash \overline{\Omega}) \end{aligned} \tag{49}$$

where D is a fixed domain in which all admissible shapes Ω are included, i.e. $\Omega \subset D$. In the present study, Φ is constructed as the signed distance function to the free boundary of a structure. Propagation of the free boundary of a structure during the course of optimization is described by the Hamilton-Jacobi equation:

$$\frac{\partial \Phi}{\partial t} + V_n = 0 \tag{50}$$

It should be noted that in the level set based method the design velocity V_n defined on the boundary Γ_O must be extended to the entire reference domain D or a narrow band around Γ_O (Sethian 1999; Osher and Fedkiw 2002). In the present work, a PDE based method (Peng et al. 1999) is used for the velocity extension. We denote the extended velocity as V_n^e. Finally, a move limit strategy (Xia et al.) is applied to V_n^e to improve the stability and convergence rate of the level set based optimization. According to the move limit strategy, V_n^e is modified as

$$\widetilde{V}_n^e(x) = V_n^e(x)\, e^{-(\Phi(x)/h)^2/\varepsilon} \tag{51}$$

where h is the grid size; ε is a parameter that controls the size of move limit, and it is set to 0.5 in the present study.

A structured grid and the finite difference method (the first order upwind spatial differencing and forward Euler time differencing) is used to solve the Hamilton-Jacobi equation. A reinitialization procedure is periodically performed. More details of the numerical computations of level set can be found in Sethian (1999), Osher and Fedkiw (2002).

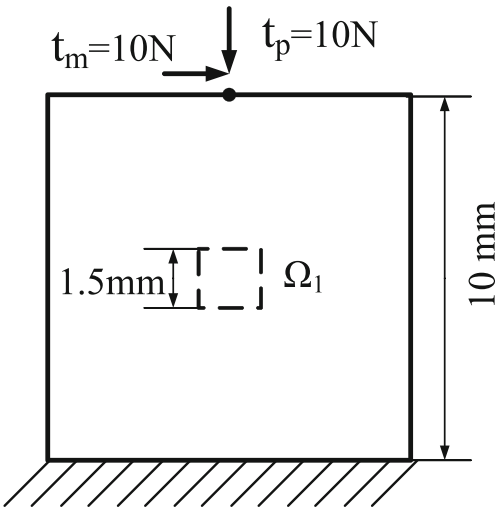

Fig. 4 Design problem of example 1

6 Numerical examples

Several examples of optimal design of piezoresistive sensors are performed in this section. In these examples, it is assumed that the solid material is the single-crystal silicon, and that the x and y axes are aligned respectively to the [110] and [$\bar{1}$10] direction of a standard (100) silicon wafer. In addition, the plane stress state is assumed, and the thickness of silicon wafer is 0.5 mm.

We do the finite element analysis by modifying a fixed background mesh and do not use the artificial weak material, as proposed in our previous study (Xia et al. 2012) and used in Xia et al. (2013). Before the optimization, we set up a background triangle mesh for the reference domain D. In each iteration of the optimization, modification of the fixed background mesh is performed to obtain a mesh that is conformal to the geometry of the structure. Linear triangle finite element is used for all the examples. The detail of the modification is referred to Xia et al. (2012).

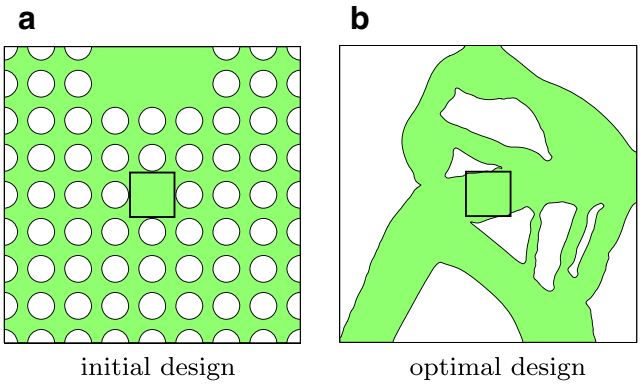

Fig. 5 The initial and optimal designs of example 1

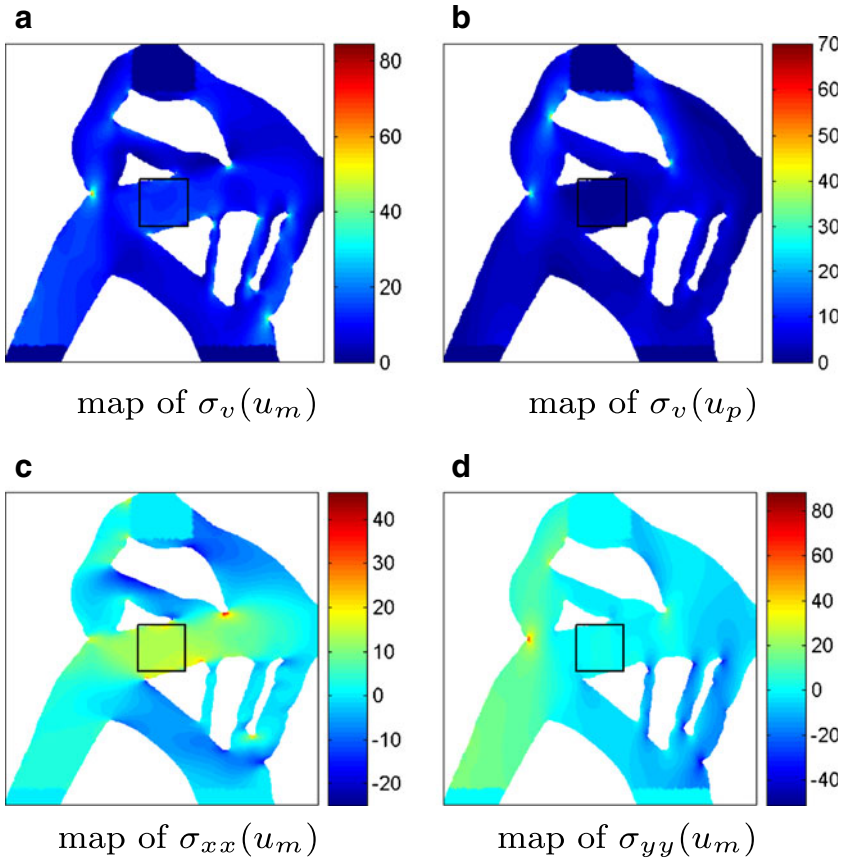

Fig. 6 Stresses of the optimal design (unit MPa)

The average absolute value of the stress differential (Xia et al. 2013) due to the measurand force t_m in the local region Ω_1, given by

$$S_m = \int_{\Omega_1} |\sigma_{xx}(u_m) - \sigma_{yy}(u_m)| \mathrm{d}x \Big/ \int_{\Omega_1} \mathrm{d}x \tag{52}$$

is computed to characterize the sensitivity of the optimal designs of the piezoresistive sensor. Similarly, the average absolute value of the stress differential due to the perturbation force t_p in the local region Ω_1, is computed to characterize cross-sensitivity

$$S_p = \int_{\Omega_1} |\sigma_{xx}(u_p) - \sigma_{yy}(u_p)| \mathrm{d}x \Big/ \int_{\Omega_1} \mathrm{d}x \tag{53}$$

Table 1 Numerical results of example 1

Design	S_m	S_p	g_0	g_1
Fig. 5b	1.3×10^7	7.8×10^5	2.0×10^7	5.6×10^5
	g_2	g_3	g_4	g_5
	5.8×10^6	2.2×10^5	1.0×10^7	1.1×10^6
Design	S_m	S_p	g_0	g_1
Fig. 7	1.4×10^7	1.5×10^6	2.1×10^7	2.8×10^5
	g_2	g_3	g_4	g_5
	2.7×10^6	1.2×10^5	–	–

6.1 Example 1

The optimal design problem of a force sensor is shown in Fig. 4. The value of the force t_m is chosen as the maximal force allowed by the sensor. The design domain is a square with width 10mm. The small square at the center of the design domain depicted by dash line are the local region Ω_1 where the piezoresistors are placed. There are 11212 linear triangle elements in the background mesh for the design domain. The parameters in the optimization are:

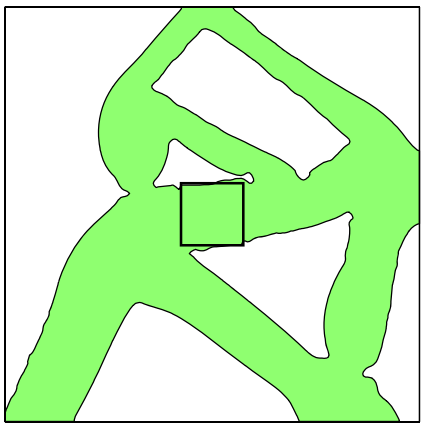

Fig. 7 The optimal design without minimizing cross-sensitivity

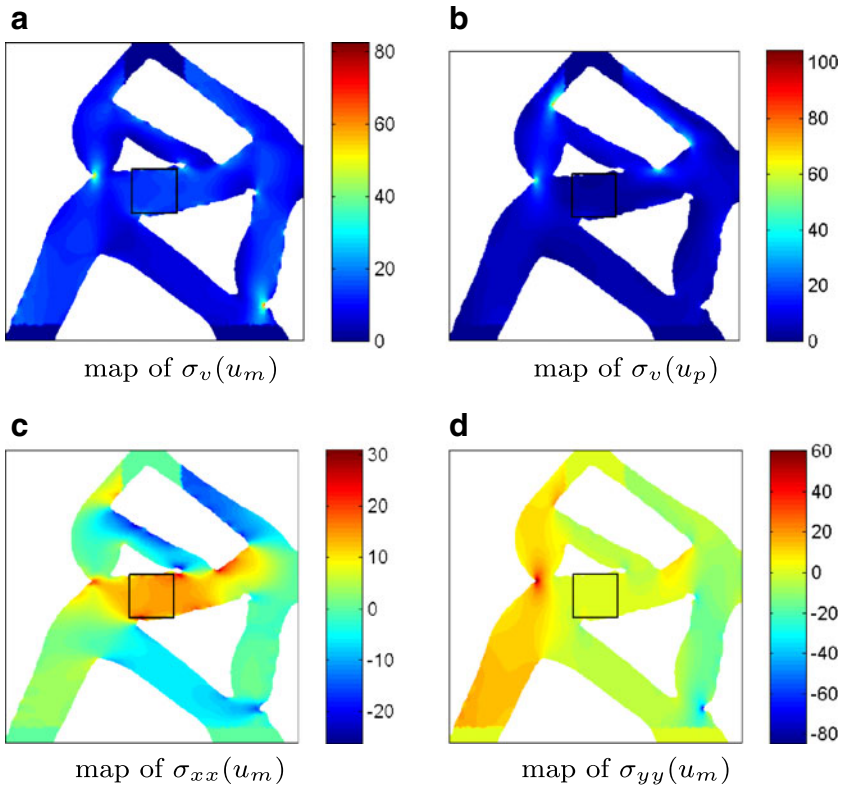

Fig. 8 Stresses of the optimal design without minimizing cross-sensitivity (unit MPa)

$\overline{\sigma}_0 = 20$MPa, $\overline{\sigma} = 15$ MPa, $\alpha = 30$, $\beta = 7 \times 10^{14}$, $w_1 = 100$, $w_2 = 1000$, $w_3 = 100$, $w_4 = 1$, $w_5 = 1000$, and Δ in the Heaviside function (Xia et al. 2012) is $\Delta = 2$ MPa. The local regions are prevented from optimization by setting the design velocity to zero for points in it. The initial design is shown in Fig. 5a.

The optimal design is shown in Fig. 5b, and the maps of stresses of the optimal design are shown in Fig. 6. Note that the high stresses in the vicinity around the point where the concentrated load is applied are not considered in the global measure of stress and is not plotted. The stress around the displacement boundary is not plotted because it may be very high at the corner. As can be seen in Fig. 6, the stresses in the local region is uniform and optimized according to our requirements. Quantitative results of the optimization are provided in Table 1, and it can be seen that the cross-sensitivity is 5.78 % of the sensitivity.

An optimization without minimizing cross-sensitivity is also performed, i.e., set $w_4 = w_5 = 0$. The optimal design is shown in Fig. 7, and the stresses of the optimal design is shown in Fig. 8. Quantitative results of the optimization

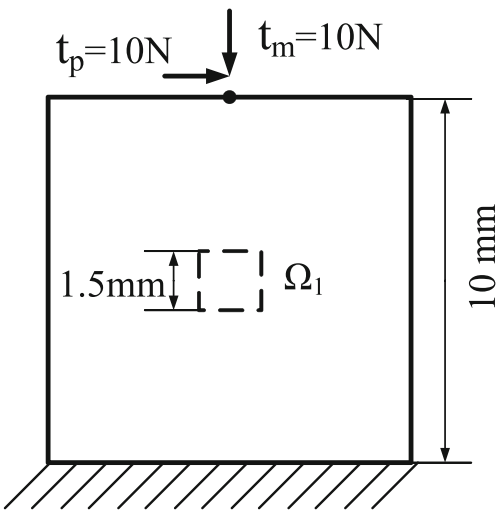

Fig. 9 Design problem of example 2

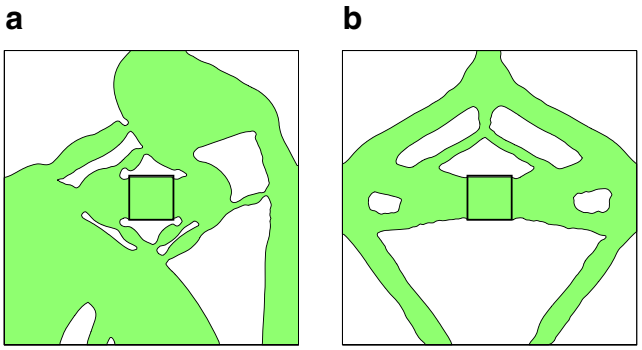

Fig. 10 The optimal designs of example 2. **a** with cross-sensitivity minimization, **b** without cross-sensitivity minimization

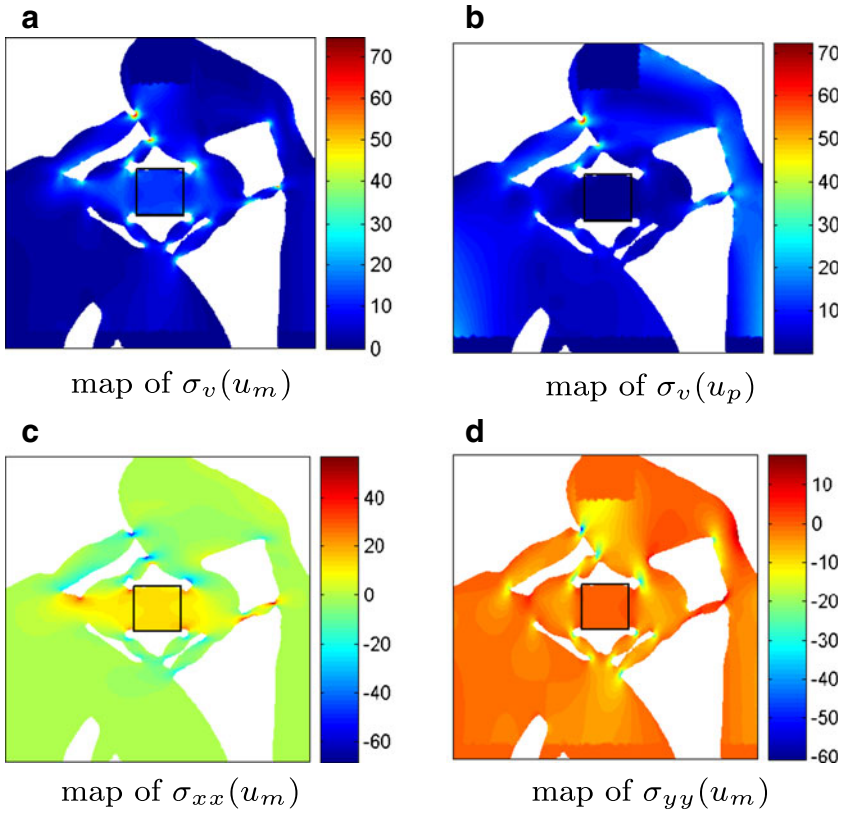

Fig. 11 Stresses of the optimal design (unit MPa)

are also provided in Table 1. It can be seen that the cross-sensitivity is 11.09 % of the sensitivity.

Comparing Fig. 7 with Fig. 5b, one can see that the shape and topology of the two designs are very similar. However, comparing the cross-sensitivity S_p of the two designs in Table 1, one can see that S_p of the design in Fig. 8 is approximately only a half of that of Fig. 7, although the sensitivity S_m of the former is a little smaller than that of the latter. According to these results, we think that the cross-sensitivity of the sensor may be significantly affected by small changes of the shape and topology of the structure. Therefore, minimizing the cross-sensitivity, together with maximizing the sensitivity, is truly necessary to improve the performance a piezoresistive sensor.

6.2 Example 2

The second example shown in Fig. 9 is very similar to the first example except that the forces t_m and t_p are swapped. The parameters in the optimization are: $\overline{\sigma}_0 = 20$MPa, $\overline{\sigma} = 15$ MPa, $\alpha = 30$, $\beta = 7 \times 10^{14}$, $w_1 = 100$, $w_2 = 1000$, $w_3 = 100$, $w_4 = 1$, $w_5 = 2000$, and Δ in the Heaviside function (Xia et al. 2012) is $\Delta = 2$ MPa. The initial design is the same as that shown in Fig. 5a.

The optimal design is shown in Fig. 10a, and the maps of stresses of the optimal design are shown in Fig. 11. As can be seen in Fig. 11, the stresses in the local region is uniform and optimized according to our requirements. Quantitative results of the optimization are provided in Table 2, and it can be seen that the cross-sensitivity is 3.78 % of the sensitivity.

An optimization without minimizing cross-sensitivity is also performed, i.e., set $w_4 = w_5 = 0$. The optimal design is shown in Fig. 10b, and the stresses of the optimal design is shown in Fig. 12. Quantitative results of the optimization are also provided in Table 2. It can be seen that the cross-sensitivity is 94.07 % of the sensitivity.

Comparing Fig. 10a with Fig. 10b, one can see that the shape and topology of the two designs are quite different. Moreover, comparing the cross-sensitivity S_p of the two designs in Table 2, one can see that S_p of the design in

Table 2 Numerical results of example 2

Design Fig. 10a	S_m	S_p	g_0	g_1
	1.3×10^7	4.7×10^5	2.1×10^7	7.6×10^5
	g_2	g_3	g_4	g_5
	7.1×10^6	1.7×10^4	2.1×10^7	1.7×10^6
Design Fig. 10b	S_m	S_p	g_0	g_1
	1.4×10^7	1.3×10^7	1.5×10^7	2.7×10^5
	g_2	g_3	g_4	g_5
	2.5×10^6	1.1×10^4	–	–

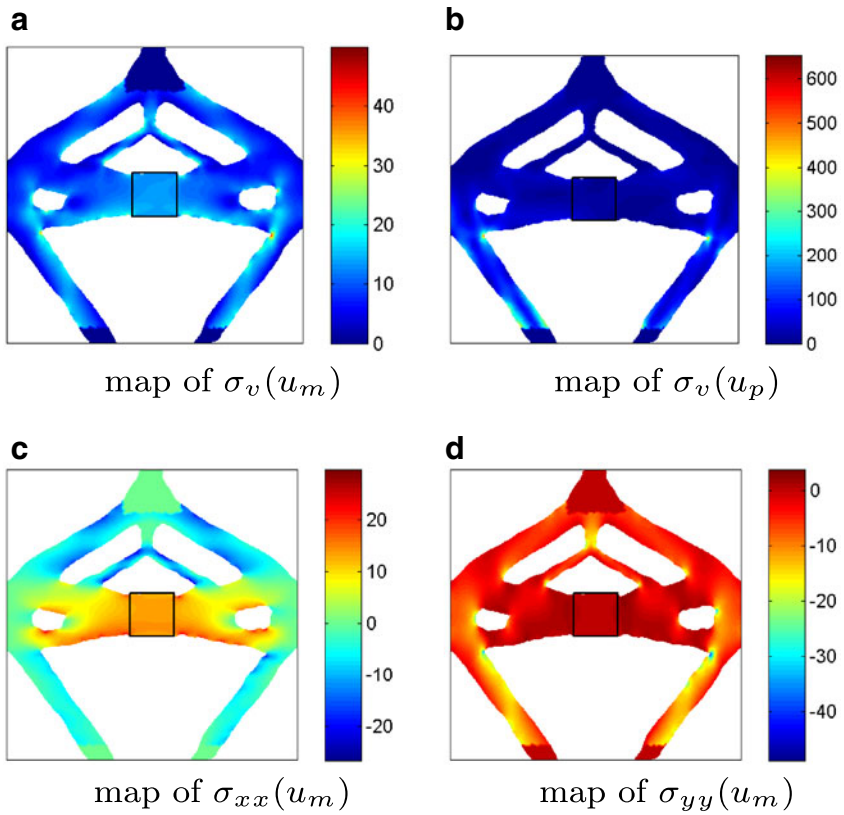

Fig. 12 Stresses of the optimal design without minimizing cross-sensitivity (unit MPa)

Fig. 10a is significantly smaller of that of Fig. 10b, although the sensitivity S_m of the former is a little smaller than that of the latter. Such results shows that it is truly necessary to consider the minimization of the cross-sensitivity in the optimal design of a piezoresistive sensor and that the proposed method is effective to maximize sensitivity and minimize cross-sensitivity.

7 Conclusion

In this paper, we presented a shape and topology optimization approach for tailoring stress in a specified local region to maximize the sensitivity and minimize the cross-sensitivity of piezoresistive sensors. Based on the analysis of a typical configuration of piezoresistive sensors, a shape and topology optimization problem is formulated. The level set method is employed to solve the optimization problem. The shape sensitivity analysis is performed via the material derivative method. Application of the method is demonstrated by several numerical examples of 2D structures. The numerical results show that it is truly necessary to consider minimization of cross-sensitivity in the optimal design of the sensors and that the method proposed in the present paper is effective to maximize the sensitivity and minimize cross-sensitivity.

Acknowledgments This research work is partly supported by the National Natural Science Foundation of China (Grant No. 51105159, 51075161), Research Fund for the Doctoral Program of Higher Education of China (Grant No. 20110142120091). The insightful comments of the reviewers' are cordially appreciated.

References

Bashir R, Gupta A, Neudeck GW, McElfresh M, Gomez R (2000) On the design of piezoresistive silicon cantilevers with stress concentration regions for scanning probe microscopy applications. J Micromech Microeng 10:483–491

Choi KK, Kim NH (2005) Structural sensitivity analysis and optimization. Springer, New York

Fratzl P, Barth FG (2009) Biomaterial systems for mechanosensing and actuation. Nature 462:442–448

Hsieh H, Chang H, Hu C, Cheng C, Fang W (2011) A novel stress isolation guard-ring design for the improvement of a three-axis piezoresistive accelerometer. J Micromech Microeng 21:105006

Kazama A, Aono T, Okada R (2013) Stress relaxation mechanism with a ring-shaped beam for a piezoresistive three-axis accelerometer. J Microelectromech Syst 22:386–394

Khaled A, Vafai K, Yang M, Zhang X, Ozkanb CS (2003) Analysis, control and augmentation of microcantilever deflections in bio-sensing systems. Sens Actuators B 94:103–115

Li L, Wang MY (2012) Stress isolation through topology optimization. In: 7th China-Japan-Korea joint symposium on optimization of structural and mechanical systems, Huangshan

Liu C (2006) Foundations of MEMS. Pearson Education, Upper Saddle River

Mei Y, Wang X (2004) A level set method for structural topology optimization and its applications. Adv Eng Softw 35:415–441

Mello LAM, Takezawa A, Silva ECN (2012) Designing piezoresistive plate-based sensors with distribution of piezoresistive material using topology optimization. Smart Mater Struct 21:085029

Mohammed AAS, Moussa WA, Lou E (2010) Optimization of geometric characteristics to improve sensing performance of MEMS piezoresistive strain sensors. J Micromech Microeng 20:015015

Osher S, Fedkiw R (2002) Level set methods and dynamic implicit surfaces. Springer-Verlag, New York

Pedersen NL (2004) On optimization of bio-probes. Int J Numer Methods Eng 61:791–806

Peng DP, Merriman B, Osher S, Zhao HK, Kang M (1999) A PDE-based fast local level set method. J Comp Phys 155:410–438

Rubio WM, Silva ECN, Nishiwaki S (2008) Piezoresistive sensor design using topology optimization. Struct Multidiscip Optim 36:571–583

Sane SP, McHenry MJ (2009) The biomechanics of sensory organs. Integr Comp Biol 49:i8–i23

Sethian JA (1999) Level set methods and fast marching methods: evolving interfaces in computational geometry, fluid mechanics, computer vision, and materials science. Cambridge monographs on applied and computational mathematics, 2nd edn. Cambridge University Press, Cambridge

Shi H, Fan S, Xing W, Li C, Sun J, Jing Z (2012) Design and fem simulation study of the electro-thermal excitation resonant beam with slit-structure. Microsyst Technol 19:979–987

Smith S (1954) Piezoresistance effect in germanium and silicon. Phys Rev 94:42–49

Takezawa A, Nishiwaki S, Kitamura M, Silva ECN (2010) Topology optimization for design strain-gauge load cells. Struct Multidiscip Optim 42:387–402

Vincent JFV, Clift SE, Menon C (2007) Biomimetics of campaniform s,ensilla; Measuring strain from the deformation of holes. J Bionic Eng 4:63–76

Wang XM, Wang MY, Guo DM (2004) Structural shape and topology optimization in a level-set framework of region representation. Struct Multidiscip Optim 27:1–19

Wang Y, Mei D, Chen Z (2011) Piezoresistive slot-cantilever type accelerometer inspired from spider's slit sensilla. Sens Lett 9:1309–1315

Xia Q, Shi T, Liu S, Wang MY (2012) A level set solution to the stress-based structural shape and topology optimization. Comput Struct 90–91:55–64

Xia Q, Shi T, Liu S, Wang MY (2013) Shape and topology optimization for tailoring stress in a local region to enhance performance of piezoresistive sensors. Comput Struct 114–115:98–105

Xia Q, Wang MY, Shi T A move limit strategy for level set based structural optimization. Eng Optim 45:1061–1072

Yang M, Zhang X, Vafai K, Ozkan CS (2003) High sensitivity piezoresistive cantilever design and optimization for analyte-receptor binding. J Micromech Microeng 13:864–872

Yang SM, Yin TI (2007) Design and analysis of piezoresistive microcantilever for surface stress measurement in biochemical sensor. Sens Actuators B 120:736–744

Zhao Y, Sun L, Liu Y, Wang W, Tian B (2012) Incorporation of the stress concentration slots into the flexures for a high-performance microaccelerometer. Rev Sci Instrum 83:075002